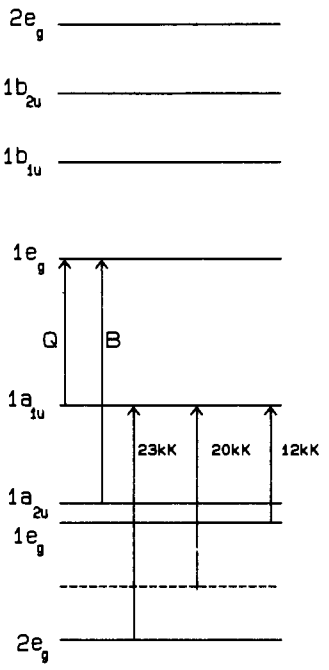

Figure 9. The molecular orbitals for $[ZnPc(-1)]^{\bullet+}$ that result in absorption between 10 000 and 45 000 cm^{-1}. The order of the orbitals is taken from the results of fitting to the spectra of ZnPc(−1)(Im).

and 23 600 cm^{-1} unaccounted for. We assign each of these bands to $\pi \rightarrow \pi$ transitions, from low-lying π MO's into the a_{1u} HOMO. The 12 200- and 23 600-cm^{-1} transitions are degenerate; the 19 500-cm^{-1} transition is nondegenerate. Acceptable transitions are as follows: $1e_g(\pi)$ or $2e_g(\pi) \rightarrow a_{1u}(\pi)$ for degenerate excited states, which should result in a Faraday *A* term, and $a_{2g}(\pi) \rightarrow a_{1u}(\pi)$, for nondegenerate excited states, which will result in *B* terms. In Figure 9 we have plotted the available molecular orbitals that represent one-electron transitions into the half-filled a_{1u} orbital, which we suggest could result in the observed MCD spectral features. Thus, we use the low-lying $1e_g$ and $2e_g$ MO's to account for the 12 170- and 23 602-cm^{-1} bands, respectively. We cannot identify, however, a nondegenerate transition to account for the 19 954-cm^{-1} band.

Conclusions

Spectral envelope deconvolution calculations can provide unambiguous data on the location and polarizations of many of the individual bands observed in spectra as complicated as those recorded for both unoxidized and oxidized metallophthalocyanines. The essential feature in these calculations is the availability of MCD data. The calculations indicate that, for complexes of ZnPc, there are five degenerate transitions, at approximately 14 900, 27 500, 29 800, 35 400, and 40 600 cm^{-1}; these transitions are associated with the Q, B, N, L, and C transitions of the Gouterman four-orbital model.

Despite extensive overlap of bands in the spectra of the oxidized $[ZnPc(-1)]^{\bullet+}$ species, the deconvolution calculations clearly indicated that a similar set of bands exists. It is suggested that the Q band is located at 14 000 cm^{-1}, with the B, N, and L bands located at 27 000, 31 500, and 36 000 cm^{-1}, respectively. Thus the Q-band energy is lower, and each of the other bands blue shifts. Bands at approximately 12 000, 19 500, and 23 600 cm^{-1} are identified as $\pi \rightarrow \pi$, into the a_{1u} HOMO. Further detailed, quantitative analyses of the spectra of oxidized phthalocyanines are needed in order to determine how general this assignment is.

Acknowledgment. We wish to acknowledge financial support from the NSERC of Canada through Operating, Strategic and Equipment grants, Imperial Oil Ltd. Canada, and the Academic Development Fund at the UWO (for an equipment grant). We are also grateful for the financial support (to T.N.) of the Canadian International Development Agency (CIDA) in conjunction with the National University of Lesotho. We wish to thank Dr. William Browett for programming assistance and Dr. Katherine Martin-Creber for carrying out preliminary studies. We are associated with the Centre for Chemical Physics at the UWO.

Contribution from the University of Pretoria,
0002 Pretoria, South Africa

Effect of Pressure on the Vibrational Spectra of Solids. 5. Raman Spectrum of Zinc Bis(pyridine) Dichloride

M. W. Venter* and A. M. Heyns

Received March 3, 1986

The effect of pressure on the Raman spectrum of $ZnCl_2(py)_2$ extenuating over the range of the internal modes of the pyridine ligand was studied. The internal vibrational modes of pyridine coordinated to the zinc tetrahedrally did not show any major differences from the vibrations of solid pyridine at low pressures. Above 10 kbar, a phase transition occurs involving changes in the C–H stretch and in-plane H-bend and out-of-plane H-bend vibrations of the ligand. The lattice region for $ZnCl_2(py)_2$ in this higher pressure phase also differs substantially from that found for this compound in the low-pressure phase, but the Raman results show that a polymeric octahedral structure is not formed. The spectral changes are explained in terms of a rotation about the Zn–N bond, which affects the Cl–H nonbonded interactions.

Introduction

Numerous vibrational studies have been carried out on complexes of the type MX_2L_2 (X = halide, L = pyridine or substituted pyridine) in an effort to assign the bands occurring in the lattice region.[1-4] Structures found include tetrahedral, square-planar, polymeric octahedral, distorted tetrahedral, and distorted polymeric octahedral ones.

One of these studies[1] found that the M–X stretching vibrations can give a good indication of the molecular symmetry present in the metal complex. The first-row transition elements of groups VIIa–IIb[5-10] (groups 7–12[11]) and Cd(II) and Hg(II)[9,10,12] all have

(1) Clark, R. J. H.; Williams, C. S. *Inorg. Chem.* **1965**, *4*, 350.
(2) Akyuz, S.; Dempster, A. B.; Davies, J. E. D.; Holmes, K. T. *J. Chem. Soc., Dalton Trans.* **1976**, 1746.
(3) Frank, C. W.; Rogers, L. B. *Inorg. Chem.* **1966**, *5*, 615.
(4) Goldstein, M.; Unsworth, W. D. *Inorg. Chim. Acta* **1970**, *4*, 342.
(5) Gill, N. S.; Nyholm, R. S.; Barclay, G. A.; Christie, T. I.; Pauling, P. J. *J. Inorg. Nucl. Chem.* **1961**, *18*, 88.
(6) Ferroni, E.; Bondi, E. *J. Inorg. Nucl. Chem.* **1958**, *8*, 458.
(7) Dunitz, J. D. *Acta Crystallogr.* **1957**, *10*, 307.

0020-1669/87/1326-1095$01.50/0

either polymeric octahedral or distorted polymeric octahedral structures, excluding Zn(II), which has a slightly distorted tetrahedral shape, and Co(II), which gives both structures.[5] If $ZnCl_2(py)_2$ were thus to assume another molecular symmetry under pressure, then the vibrational spectrum of the M–X stretching modes should indicate this quite clearly.

The vibrational spectra of $ZnCl_2(py)_2$ have been extensively studied and include pressure studies up to 12 kbar.[13]

Since the previous studies did not report any phase transition in $ZnCl_2(py)_2$, the present work deals mainly with the spectral changes at the phase transition in this compound and also with a possible mechanism for the transition. In samples that were not properly dried, the phase transition occurred at higher pressures, i.e. ~17 kbar at ambient temperatures, and for this reason has not been detected in a previous Raman high-pressure study to 12 kbar. Earlier high-pressure studies also made no mention of the internal vibrations of the pyridine molecule. Definite changes occurred in these modes at higher pressure and have therefore been included in this study.

Experimental Section

The $ZnCl_2(py)_2$ complex was isolated from ethanolic solutions of pyridine and $ZnCl_2$, and the product was crystallized from ethanol, dried under vacuum, and stored in a desiccator over P_2O_5. C, H, N, and Zn analyses were found to be satisfactory, the Raman spectra were recorded on a Spex Model 1403 instrument, and the diamond anvil cell[14] was used for the pressure study. More complete details of the methods followed, instrumentation, and design of the experiment are given elsewhere.[15]

Crystal Structure and Symmetry-Allowed Vibrations

The crystal structure of $ZnCl_2(py)_2$ is given by the space group $P2_1/c$ (C_{2h}^5) with $Z = 4$.[16,17] Accordingly, $3A_g + 3B_g$ translational, $3A_g + 3B_g$ rotational, and $9A_g + 9B_g$ skeletal Raman-active vibrations of $ZnCl_2(py)_2$ should be obtained in the lattice region. The crystal structure indicates that two types of pyridine rings are present. It is thus expected that all vibrational modes involving zinc and the pyridine rings should be split. This multiplicity is however not observed in any of the Raman studies cited. Also of interest, is the fact that the Cl–Zn–Cl angle (120.9°) is larger and the N–Zn–N angle (106.3°) smaller than those obtained for perfect tetrahedra. The Zn–Cl distances are also longer than any of the analogous bond lengths in the 4-substituted pyridine series.[18] These significant differences are attributable to some Cl---H nonbonded interactions.[16,17]

A total of 30 bands should thus be observed in the Raman spectrum of the lattice region of $ZnCl_2(py)_2$. Due to the limitations of the instrument used, only vibrations occurring above ~50 cm^{-1} could be observed. Although only eight bands were obtained in this region, it must be noted that some of these were broad, and previous authors had assigned these to more than one mode.[13] The frequencies and approximate intensities were found on the whole to be comparable to those reported by the above-mentioned authors.

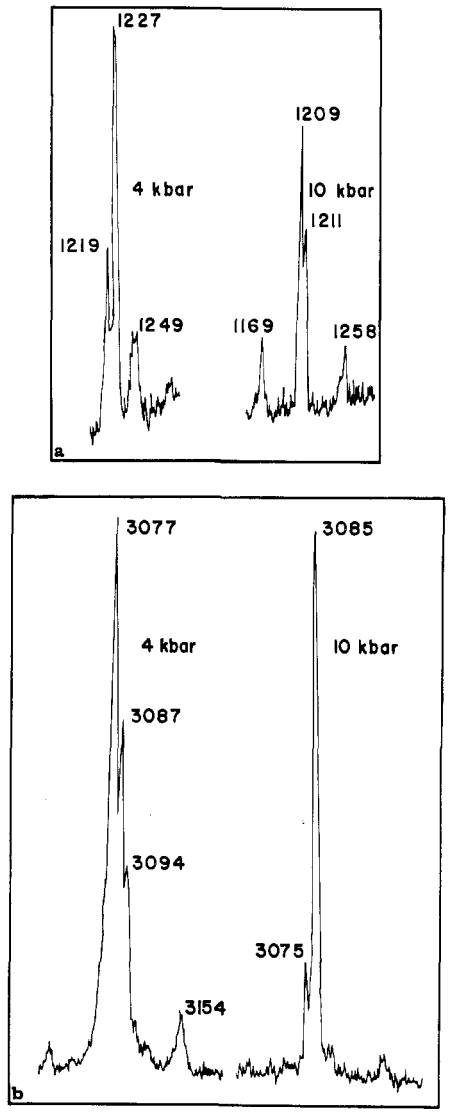

Figure 1. (a) C–H bending modes of $ZnCl_2(py)_2$. (b) C–H stretching modes of $ZnCl_2(py)_2$.

Results and Discussion

Below 10 kbar, the effect of pressure on the internal modes of pyridine complexed tetrahedrally to the zinc is similar to the results obtained for uncoordinated pyridine at low pressures.[15] At the same pressures, the ν values for $ZnCl_2(py)_2$ were approximately 20 cm^{-1} higher on average than those for uncoordinated pyridine. Above 10 kbar, the spectrum undergoes marked changes in some of the internal modes of coordinated pyridine (Figure 1). It is also evident in Figure 2 that the lattice modes change even more profoundly. If the $ZnCl_2(py)_2$ complex were to undergo a transition from tetrahedral to polymeric octahedral, then a large downward shift in frequency should be observed in the M–Cl modes, as bridging M–Cl skeletal modes are found at lower frequencies than terminal M–Cl modes; e.g. for $CoCl_2(py)_2$ the monomeric tetrahedral species has Co–Cl terminal stretches at 347 and 306 cm^{-1} whereas the $CoCl_2(py)_2$ polymeric octahedral species has the bridged Co–Cl stretching modes at much lower frequencies, i.e. 186 and 174 cm^{-1}.[19] The Zn–Cl stretching mode shifted from 299 cm^{-1} (4 kbar) to 311 cm^{-1} (10 kbar), i.e. an upward shift of frequency with pressure. Since no shift toward lower wavenumbers was observed in the zinc complex, this type of structural transition was discounted. Some structural changes must thus have occurred within the tetrahedral arrangement of

(8) Morosin, B. *Acta Crystallogr., Sect. B: Struct. Crystallogr. Cryst. Chem.* **1975**, *B31*, 632.
(9) McConnell, A. A.; Nuttall, R. H. *J. Mol. Struct.* **1978**, *49*, 207.
(10) Zannetti, R.; Serra, R. *Gazz. Chim. Ital.* **1960**, *90*, 328.
(11) The periodic group notation in parentheses is in accord with recent actions by IUPAC and ACS nomenclature committees. A and B notation is eliminated because of wide confusion. Groups IA and IIA become groups 1 and 2. The d-transition elements comprise groups 3 through 12, and the p-block elements comprise groups 13 through 18. (Note that the former Roman number designation is preserved in the last digit of the new numbering: e.g., III → 3 and 13.)
(12) (a) Paulus, V. H. *Z. Anorg. Allg. Chem.* **1969**, *369*, 38. (b) Barr, R. M.; Goldstein, M.; Unsworth, W. D. *J. Cryst. Mol. Struct.* **1974**, *4*, 165.
(13) Wong, P. T. T. *J. Chem. Phys.* **1975**, *63*, 5108.
(14) Hawke, R. S.; Syassen, K.; Holzapfel, W. S. *Rev. Sci. Instrum.* **1974**, *45*, 1598.
(15) Heyns, A. M.; Venter, M. W. *J. Phys. Chem.* **1985**, *89*, 4546.
(16) Sokolova, Yu. A.; Atovmyan, L. O.; Porai-Koshits, M. A. *J. Struct. Chem. (Engl. Transl.)* **1965**, *7*, 794.
(17) Steffen, W. L.; Palenik, G. J. *Acta Crystallogr., Sect. B: Struct. Crystallogr. Cryst. Chem.* **1976**, *B32*, 298.
(18) Steffen, W. L.; Palenik, G. J. *Inorg. Chem.* **1977**, *16*, 1119.
(19) Postmus, C.; Ferraro, J. R.; Quattrochi, A.; Shobatake, K.; Nakamoto, K. *Inorg. Chem.* **1969**, *8*, 1851.

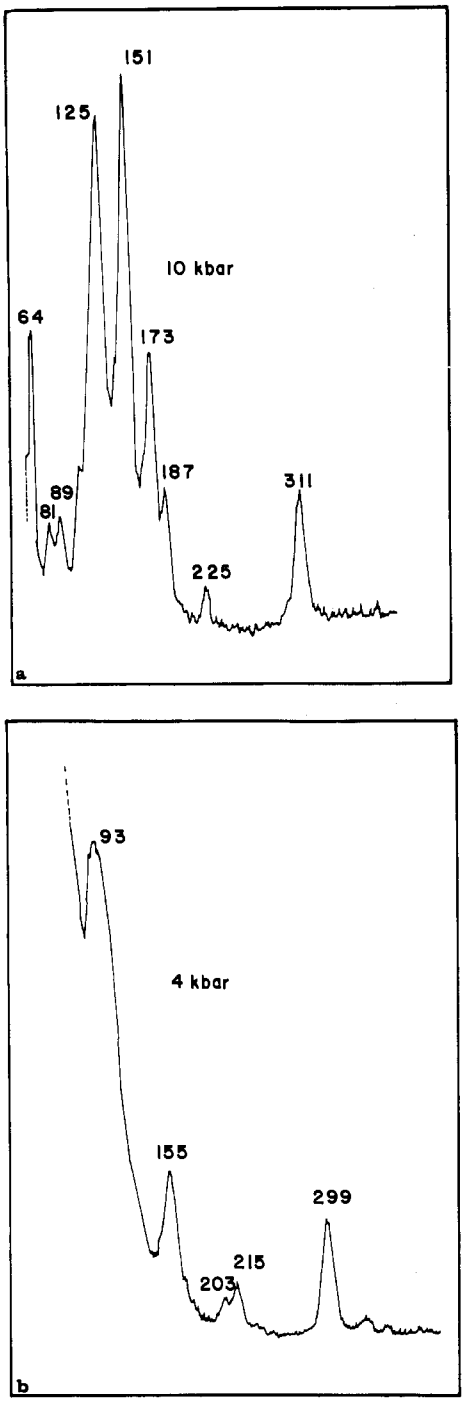

Figure 2. (a) Lattice modes of $ZnCl_2(py)_2$ at 10 kbar. (b) Lattice modes of $ZnCl_2(py)_2$ at 4 kbar.

the $ZnCl_2(py)_2$ molecule. A careful analysis of both the skeletal modes of $ZnCl_2(py)_2$ as well as the internal modes of the pyridine ring itself is thus required.

In the case of the internal pyridine modes, the regions most severely affected are the C–H bending (1200 cm^{-1}) and the C–H stretching (3000 cm^{-1}) regions. In the C–H bending region (Figure 1a), a large downward shift is obtained in the two largest peaks; i.e., the energy of the bending modes has been lowered. In the C–H stretching region a large upward shift of the most intense peak is obtained, which implies a shortening of the C–H bond length. It must also be noted that the two shoulders at higher frequencies disappeared, with the simultaneous appearance of one peak at lower frequency (Figure 1b). This spectrum of the higher pressure phase in the C–H region is characteristic of pyridine complexes with no hydrogen bonding.[18] If the hydrogen bonds between Cl and H were to be broken, then one would expect

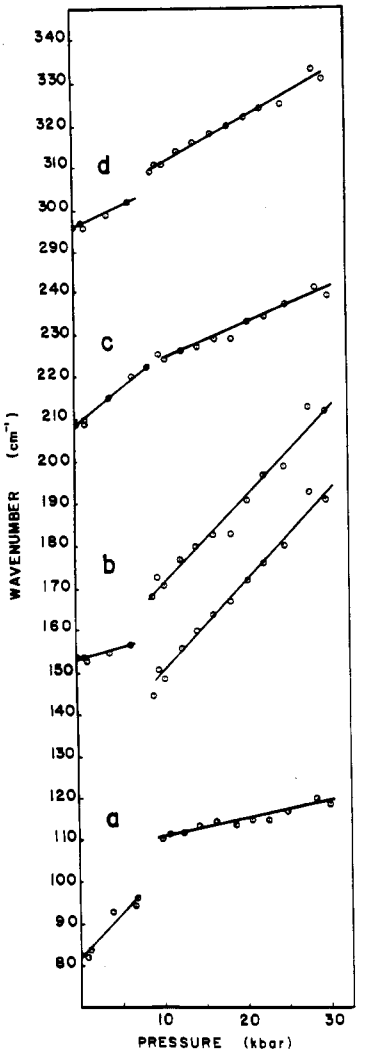

Figure 3. Pressure dependence of $ZnCl_2(py)_2$ lattice modes: a = δ(N–Zn–N), δ(Cl–Zn–N); b = ν(Zn–N), ν(lattice), δ(Cl–Zn–N), δ(lattice); c = ν(Zn–N), ν(Zn–Cl), δ(Cl–Zn–Cl); d = ν(Zn–N), δ(Cl–Zn–N).

changes in the internal C–H modes as well as in the Zn–Cl skeletal modes. It has already been established that the Zn–Cl vibrational modes of the unsubstituted pyridine complex do not agree with the values obtained for $(4\text{-R-py})_2ZnCl_2$ type complexes, which do not have any intermolecular Cl---H contacts. This is a clear indication that the Cl---H contacts that occur intermolecularly via the para position of the pyridine ring influence the Zn–Cl bond length to a larger extent than the intramolecular Cl---H contacts that occur via the hydrogen atoms on the ortho positions of the pyridine ring. If the Zn–Cl vibrations were to agree with the results obtained for the 4-substituted pyridine complexes, then the vibrations should be obtained at higher frequencies than those obtained under ambient conditions. Apart from the normal pressure shifts,[20] the Zn–Cl skeletal modes undergo a large shift toward higher ν values at the phase transition; this is also observed in the C–H stretching modes as mentioned earlier. A similar shift in the Zn–N skeletal modes is not observed. This effect corresponds to a substantial shortening of both the Zn–Cl and C–H bond lengths and thus less intermolecular Cl---H interaction. The phase change must thus have involved a diminishing Cl---H bonding effect.

The peaks obtained below 200 cm^{-1} undergo the most changes (Figure 3). The assignments for these differ among the various authors.[13,21-23] The vibration obtained at 154 cm^{-1} splits into two

(20) Sherman, W. F. *Bull. Soc. Chim. Fr.* **1982**, *I-297*, I-347.
(21) Postmus, C.; Ferraro, J. R.; Wozniak, W. *Inorg. Chem.* **1967**, *6*, 2030.
(22) Saito, Y.; Cordes, M.; Nakamoto, K. *Spectrochim. Acta, Part A* **1972**, *28A*, 1459.
(23) Nakamoto, K. *Angew. Chem., Int. Ed. Engl.* **1972**, *11*, 666.

bands at high pressures, both of which give the same magnitude of shift with pressure (Figure 3); these shifts are large, and it is suggested that a librational mode is included in this feature.[13] Since all the skeletal modes involving Zn–Cl bond stretches and Zn–Cl bending modes, as well as the pyridine ring rotational modes, would be expected to undergo changes at higher pressures, it is difficult to assign the lattice and skeletal modes in the higher pressure phase. Frequency shifts of the lattice modes with pressure are usually large,[20] and it can therefore be assumed that vibrations at low wavenumbers have now moved into the frequency range observable by the instrument used, thus further complicating the low-frequency spectrum. At this stage thus, no assignment in this region can be given.

Conclusion

The application of pressure on a hydrogen-bonded compound usually results in an increase in the hydrogen-bonded contacts.[20] This should cause the C–H and Zn–Cl stretching modes to shift downward, since they are weakened by the increasing strength of the H---Cl bond. This however has been found not to be the case for $ZnCl_2(py)_2$, as the stretching modes shift upward. The Zn–Cl bond length is thus shortened, resulting in higher frequency Zn–Cl stretching modes. Similarly, a reduction of H bonding resulted in shorter C–H bond lengths and lower frequency C–H bending vibrations. Since these are the only internal pyridine vibrations that undergo any dramatic changes at the phase transition, it is thought that a rotation about the Zn–N bond takes place above 10 kbar with a corresponding reduction in the Cl---H nonbonded interactions. If the phase transition does indeed primarily involve a change in the strength of the hydrogen bonds, the profound effect that moisture has on the transition pressure, as mentioned earlier, can easily be understood. Finally, the Zn(II) ion was found to be too small to form the polymeric octahedral structure, even up to pressures of 30 kbar.

Acknowledgment. We thank the University of Pretoria and the CSIR, Pretoria, for financial assistance.

Registry No. $ZnCl_2(py)_2$, 6843-20-5.

Supplementary Material Available: Tables of the wavenumbers and pressure dependence of the lattice modes and the internal pyridine modes of $ZnCl_2(py)_2$ (2 pages). Ordering information is given on any current masthead page.

Contribution No. 7454 from the Arthur Amos Noyes Laboratory, California Institute of Technology, Pasadena, California 91125

Electronic and Vibrational Spectra of $Ru_2(carboxylate)_4^+$ Complexes. Characterization of a High-Spin Metal–Metal Ground State

Vincent M. Miskowski,* Thomas M. Loehr,† and Harry B. Gray*

Received August 7, 1986

Solid-state near-infrared absorption spectra at low temperature have been obtained for eight compounds containing [Ru_2(carboxylate)$_4$X] chains or [Ru_2(carboxylate)$_4X_2$]$^-$ units (carboxylate is acetate, propionate, or *n*-butyrate), including single-crystal data for six compounds. The $\delta \rightarrow \delta^*$ transition is assigned to a band with a completely molecular *z*-polarized origin near 9000 cm^{-1}. Sharp vibronic structure has been interpreted with the aid of detailed vibrational studies. Butyrates show predominant *z*-polarized structure in an excited-state $\nu(Ru_2)$ of ~300 cm^{-1}, along with weak vibronic origins built on a_{1g} ν(RuO) at 430 cm^{-1} and $\delta(CO_2)$ at ~700 cm^{-1}. Propionates are similar, but ν(RuO) is at ~400 cm^{-1}, whereas acetates show strong progressions in both $\nu(Ru_2)$ and ν(RuO), the latter at ~360 cm^{-1}. The unusual vibronic effect is attributed to strong ground-state coupling of the a_{1g} ν(RuO) and $\nu(Ru_2)$ modes in the acetates. Weak, *x*,*y*-polarized absorption is observed for all compounds built on e_g vibronic origins at ~250 cm^{-1} ($\delta(RuO_2)$), ~310 cm^{-1} (ν(RuO)), and ~1450 cm^{-1} (symmetric $\nu(CO_2)$). Franck–Condon factors for progressions in a_{1g} modes built on the e_g vibronic origins are very different from those in the *z*-polarized spectrum. A very weak ($\epsilon \sim 1$–5) absorption with an electronic origin at ~6900 cm^{-1}, which exhibits molecular *x*,*y* polarization and a single long progression in $\nu(Ru_2)$ (~340 cm^{-1}), is assigned to the spin-forbidden $\pi^* \rightarrow \delta^*$ transition. In addition, two very weak and narrow peaks at 5048 (observed in absorption for one compound) and ~1600 cm^{-1} (observed in resonance Raman) are tentatively assigned to spin-flip transitions within the $(\pi^*,\delta^*)^3$ configuration.

Molecules containing metal–metal quadruple bonds often exhibit vibronic structure in the $\delta \rightarrow \delta^*$ absorption system.[1-3] The study of these systems is of great interest, because the vibronic structure contains considerable information about the metal–metal interaction. Particularly for carboxylate-bridged metal dimers, this interaction is not simply described.[4]

The diruthenium(II,III) carboxylates, $Ru_2(O_2CR)_4^+$, have a spin-quartet ground state.[5] Norman and co-workers[4] explained this ground state in terms of the pattern of metal–metal-bonding and -antibonding orbitals characteristic of strong metal–metal interactions. The diruthenium(II,III) compounds possess 3 electrons in excess of the 8 required for a metal–metal quadruple bond. The lowest energy metal–metal-antibonding orbitals, π^* and δ^*, turn out to be nearly degenerate. Thus, a high-spin $\sigma^2\pi^4\delta^2(\delta^*)^1(\pi^*)^2$ ground state is adopted.

Complexes with this ground state should display all of the electronic transitions characteristic of quadruply bonded dimers, including the $\delta \rightarrow \delta^*$ transition. Our investigation of this transition has centered mainly on the $Ru_2(O_2CR)_4X$ (X = halide) compounds, because in these chain-structured materials the chromophore orientation is often exceptionally favorable for single-crystal polarized electronic spectroscopy. We have found well-resolved vibronic structure in the $\delta \rightarrow \delta^*$ absorption systems of several $Ru(O_2CR)_4^+$ species, and it has been interpreted with the aid of ground-state vibrational spectroscopic studies.

† Oregon Graduate Center, Beaverton, OR 96006.

(1) (a) Trogler, W. C.; Gray, H. B. *Acc. Chem. Res.* **1978**, *11*, 232. (b) Hopkins, M. D.; Gray, H. B. *J. Am. Chem. Soc.* **1984**, *106*, 2468.
(2) (a) Martin, D. S.; Newman, R. A.; Fanwick, P. E. *Inorg. Chem.* **1979**, *18*, 2511. (b) Martin, D. S.; Newman, R. A.; Fanwick, P. E. *Inorg. Chem.* **1982**, *21*, 3400. (c) Huang, H. W.; Martin, D. S. *Inorg. Chem.* **1985**, *24*, 96.
(3) (a) Cotton, F. A.; Walton, R. A. *Multiple Bonds Between Metal Atoms*; Wiley: New York, 1982; Chapter 8. (b) Cotton, F. A.; Fanwick, P. E.; Gage, L. D. *J. Am. Chem. Soc.* **1980**, *102*, 1570.
(4) (a) Norman, J. G., Jr.; Kolari, H. J.; Gray, H. B.; Trogler, W. C. *Inorg. Chem.* **1977**, *16*, 987. (b) Norman, J. G., Jr.; Kolari, H. J. *J. Am. Chem. Soc.* **1978**, *100*, 791. (c) Norman, J. G., Jr.; Renzoni, G. E.; Case, D. A. *J. Am. Chem. Soc.* **1979**, *101*, 5256.
(5) (a) Stephenson, T. A.; Wilkinson, G. *J. Inorg. Nucl. Chem.* **1966**, *28*, 2285. (b) Mitchell, R. W.; Spencer, A.; Wilkinson, G. *J. Chem. Soc., Dalton Trans.* **1973**, 846.

0020-1669/87/1326-1098$01.50/0